

# Regularization of the collision in the electromagnetic two-body problem

Efraim Buksman Hollander and Jayme De Luca

Universidade Federal de São Carlos,

Departamento de Física

Rodovia Washington Luis, km 235

Caixa Postal 676, São Carlos,

São Paulo 13565-905

(Dated: February 9, 2020)

## Abstract

We derive a differential equation that is regular at the collision of two equal-mass bodies with attractive interaction in the relativistic action-at-a-distance electrodynamics. Our method uses the energy constant related to the Poincaré invariance of the theory to motivate the regularizing coordinate transformation and to remove infinities from the equation of motion. The collision orbits are calculated numerically using the regular equation adapted in a self-consistent minimization method (a stable numerical method that chooses only nonrunaway solutions). This dynamical system appeared 100 years ago as a time-symmetric relativistic motion and acquired the status of electrodynamics in the 1940's by the works of Dirac, Wheeler and Feynman. We outline the method with an emphasis on the physics of this complex conservative dynamical system. In particular we compare the regularization of this Poincaré invariant problem to the Levi-Civita regularization of the Galilei invariant Kepler problem.

---

corresponding author; email address: deluca@df.ufscar.br

## I. INTRODUCTION

A difficulty with the numerical calculation of an orbit for the relativistic two-body problem with attractive interaction is the collision, where the delay equation of motion in the usual form becomes singular. This obstacle has so far prevented the numerical study of this problem. In this work we derive a delay differential equation that is regular at the collision of two equal-mass bodies with attractive interaction in the action-at-a-distance electrodynamics. We use the constant energy related to the Poincaré invariance of this dynamical system [13] to remove infinities from the equation of motion, analogously to the Levi-Civita regularization of the Kepler problem [46]. The regular equation of motion is adapted in a numerical method previously developed by us for the repulsive problem [7]. This method postulates future and past histories and finds the self-consistent orbit by integrating two regular motions followed by a minimization scheme to make the two histories consistent. We calculate numerically collision orbits with energies ranging from the nuclear to the atomic scale. As the physical motivation, the reader should keep the collision dynamics of the Kepler problem in mind, which is the non-relativistic analogous to our problem.

In 1903, Schwarzschild proposed a relativistic type of interaction between charges that is time reversible precisely because it involves retarded and advanced interactions symmetrically [8]. The same model reappeared in the 1920s in the work of Tetrode and Fokker [9] and it finally became an interesting physical theory after Wheeler and Feynman showed that this direct-interaction theory can describe all the classical electromagnetic phenomena (i.e. the classical laws of Coulomb, Faraday, Ampère, and Biot-Savart) [1, 10]. Wheeler and Feynman also showed in 1945 that in the limit where the electron interacts with a completely absorbing universe, the response of this universe to the electron's field is equivalent to the local Lorentz-Dirac self-interaction theory [11] without the need of mass renormalization [1]. It is amusing to understand the classical radiative phenomena of Maxwell's electrodynamics as a limiting case of this direct-interaction theory (complete absorption is added to the theory as an approximation to uncouple away from the detailed neutral-delay dynamics of the other charges of the universe; for other approximations see [12]). The Wheeler and Feynman program [13] to quantize the action-at-a-distance electrodynamics as a means to

overcome the infinities of QED is still not implemented because of the lack of a Hamiltonian description. Some progress was achieved recently in [7], where we developed a simple finite-dimensional Hamiltonian description for the electromagnetic two-body problem with repulsive interaction. The generalization to the attractive case involves regularization, which was a motivation for the present work.

The isolated two-body system, away from the other charges of the universe is a conservative time-reversible dynamical system in the action-at-a-distance electrodynamics. We consider here only the equal-mass two-body system ( $m_1 = m_2 = m$ ), henceforth called 1D-WF2B. The only postulate of the relativistic action-at-a-distance electrodynamics is that the equations of motion be derived formally [14] by extremizing the parametrization-independent action

$$S_F = \int m ds_1 + \int m ds_2 - \frac{e_1 e_2}{2} \int \int (\dot{x}_1 - \dot{x}_2) \cdot \dot{x}_1 \dot{x}_2 ds_1 ds_2; \quad (1)$$

where  $x_i(s_i)$  represents the four-position of particle  $i = 1, 2$  parametrized by its arc-length  $s_i$ , double bars stand for the four-vector modulus  $\|\dot{x}_1 - \dot{x}_2\| = \sqrt{(\dot{x}_1 - \dot{x}_2) \cdot (\dot{x}_1 - \dot{x}_2)}$ , and the dot indicates the Minkowski scalar product of four-vectors with the metric tensor  $g$  ( $g_{00} = 1; g_{11} = g_{22} = g_{33} = -1$ ) (the speed of light is  $c = 1$ ). The attractive problem is defined by Eq.(1) with  $e_1 = -e_2 = e$  (positronium atom), while the repulsive two-electron problem is defined by Eq.(1) with  $e_1 = e_2 = e$ . For the repulsive two-electron problem along symmetric orbits [ $\dot{x}_2(t) = \dot{x}_1(t) - \dot{x}(t)$ ], minimization of action (1) prescribes the following equation of motion

$$m \frac{d}{dt} \left( \frac{\dot{x}}{1 - v^2} \right) = \frac{e^2}{2r^2} \frac{1 - v(t-r)}{1 + v(t-r)} + \frac{e^2}{2q^2} \frac{1 + v(t+q)}{1 - v(t+q)}; \quad (2)$$

where  $v(t) = dx/dt$  is the velocity of the first electron, of mass  $m$  and charge  $e$ , and  $r$  and  $q$  are the time-dependent delay and advance, respectively. The functions  $r(t)$  and  $q(t)$  are implicitly defined by the light-cone conditions

$$r(t) = x(t) + x(t-r); \quad (3)$$

$$q(t) = x(t) + x(t+q);$$

In general, a neutral-delay equation such as Eq. (2) requires a pair of world-line segments as the initial condition (one world-line segment for each particle). As discussed in Ref. [15], the initial world-line segments can be provided in such a way that Eq.(2) is well-posed, by using "maximal independent segments". A pair of world-line segments is called independent

if the end points of each segment lie on the forward and backward light-cones of a single point interior to the other segment. Last, a surprising existence theorem was proved for the symmetric motion of two electrons along a straight line [  $x_2(t) = x_1(t) - x(t)$  (Eq. (2)) ]. It is shown in Ref. [16] that for sufficiently low energies, initial conditions of Newtonian type [  $x(0) = x_0$  and  $v(0) = v_0$  ] determine the unique solution that is globally defined (i.e., that does not runaway at some point) [16]. Existence/uniqueness proofs are still lacking for the case of attractive interaction, and we hope that with the present regularization of the equation of motion such proofs can be facilitated.

For this electromagnetic two-body problem, the only known analytical solution is the circular orbit for the attractive problem [17, 18] (see also [19] for the stability analysis of circular orbits). The first numerical method to solve Eq.(2) was developed in [20] and converged to solutions up to  $v=c = 0.94$ : Later another method [21] converged up to  $v=c = 0.99$ . In reference [7] we developed a numerical method to find non-runaway solutions for the repulsive problem. This method is based on minimization and it avoids integration of the delay equation. Precisely because of the singularity, numerical methods and studies for the attractive problem are lacking, and the method developed in [22] can not deal with a near-collision. We hope that this work can start to fill this gap and here we use the regular equation of motion adapted in a method developed by us in Ref.[7]. This paper is organized as follows: In section II we build up familiarity with the collision orbit and regularization issues. In section III we study the behavior of the symmetric orbit near the collision, and we introduce the motivation for a change of the evolution parameter. Section IV discusses the energy related to the Poincare invariance of the theory. The expression of this energy motivates the definition of two finite variables that are used in the regular differential equation. In Section V we adapt the regular equation in a numerical method that integrates future and past histories until the eventual self-consistency of these two histories. In this section we also discuss the numerical calculation of the orbit in several energy ranges, and discuss the implementation needed in each range to speed up convergence of the method. In section VI we put the conclusion and discussions. Appendix A discusses the Levi-Civita regularization and stresses some topological differences between our Poincare invariant case and the Galilei invariant Kepler problem.

## II. PRELIMINARIES TO THE REGULARIZATION

The motivation for our regularization of the attractive problem is the Levi-Civita regularization of the Kepler problem [5, 6], which we discuss in Appendix A. We henceforth use a unit system where  $m = c = e_1 = e_2 = 1$ . We assume that at  $t = t_c$  particle 1 is at  $x_1 = 0$  and moving to the right while particle 2 is at the same point and moving to the left (outgoing collision). The particles collide again at  $t = t_c$  with ingoing velocities, so that  $\dot{x}_1(t) > 0$  and  $\dot{x}_2(t) < 0$  all along the unit cell of our orbit (see Figure 1). We further restrict attention to symmetric colinear motion, where the trajectories of particles 1 and 2 satisfy

$$\dot{x}_1(t) = -\dot{x}_2(t) : \quad (4)$$

It turns out, for the equal mass case only, that the symmetric orbit is defined in any Lorentz frame by the covariant condition that the future of particle 1 is the past of particle 2; as explained in Appendix B of Ref. [7]. Because the transformations involved in the regularization are elaborate, we choose to work in the special Lorentz frame where the orbit is symmetric and therefore we lose covariance in benefit of the intuitive picture. A covariant analysis shall be left for later work.

As seen with Eqs. (2) and (3), the electrodynamic interaction connects points that are in light-cone condition, as defined by

$$\begin{aligned} r_a &= \dot{x}_1(t_1) - \dot{x}_2(t_{2a}) = c(t_{2a} - t_1); \\ r_b &= \dot{x}_1(t_1) - \dot{x}_2(t_{2b}) = c(t_1 - t_{2b}); \end{aligned} \quad (5)$$

In the above, subscripts a and b indicate future and past times of particle 2 in light-cone to the present time  $t_1$  of particle 1 (see Figure 2). By use of Eq. (5), we can express  $t_{2a}$  and  $t_{2b}$  as

$$\begin{aligned} t_{2a} &= t_1 + r_a/c; \\ t_{2b} &= t_1 - r_b/c; \end{aligned} \quad (6)$$

and from Eqs. (5) and (6) we can also derive the equation of motion for  $t_{2a}$

$$\frac{dt_{2a}}{dt_1} = \frac{(1 + v_1)}{(1 + v_{2a})} : \quad (7)$$

The equation of motion for particle 1 in the attractive 1D-WF2B can be obtained from Eq. (2) by changing the sign of the right-hand side, performing a trivial algebraic manipulation on the left-hand side and setting  $m = e^2 = 1$ , yielding

$$\frac{dv_1}{dt_1} = \frac{1}{2} \left[ \frac{1}{r_a^2} \frac{(1 - v_{2a})}{(1 + v_{2a})} + \frac{1}{r_b^2} \frac{(1 + v_{2b})}{(1 - v_{2b})} \right] \frac{1}{v_1^3} : \quad (8)$$

The symbols  $v_{2b}$  and  $v_{2a}$  in Eq. (8) stand for the retarded and advanced velocities of particle 2, which along symmetric orbit satisfying Eq. (4) are defined from the velocity  $v_1(t)$  of particle 1 by

$$\begin{aligned} v_{2a}(t) &= v_1(t + r_a = c); \\ v_{2b}(t) &= v_1(t - r_b = c); \end{aligned} \quad (9)$$

as illustrated in Figure 2. In the same way that we derived Eq. (7), the motion of  $x_{2a}$ ,  $x_{2b}$ ,  $t_{2a}$  and  $t_{2b}$  can be derived from Eqs. (5) and (6) as well, completing the system of equations to be added to Eq. (8)

$$\frac{dx_1}{dt_1} = v_1; \quad (10)$$

$$\frac{dt_{2a}}{dt_1} = \frac{(1 + v_1)}{(1 + v_{2a})}; \quad (11)$$

$$\frac{dx_{2a}}{dt_1} = v_{2a} \frac{(1 + v_1)}{(1 + v_{2a})}; \quad (12)$$

$$\frac{dt_{2b}}{dt_1} = \frac{(1 - v_1)}{(1 - v_{2b})}; \quad (13)$$

$$\frac{dx_{2b}}{dt_1} = v_{2b} \frac{(1 - v_1)}{(1 - v_{2b})}; \quad (14)$$

By use of Eqs. (4) and (5), we can show that along symmetric orbits the two quantities  $r_a(t_1)$  and  $r_b(t_1)$  are defined by a single function  $r(t)$  as

$$\begin{aligned} r_a(t) &= r(t); \\ r_b(t + r_a = c) &= r(t); \end{aligned} \quad (15)$$

which is illustrated in Fig. 3. As the force is always attractive from both retarded and advanced positions in Eq. (8), after the velocities have switched opposite the interparticle distance must approach zero until the collision happens. We shall start by showing that

both velocities must tend to the speed of light as the particles approach the collision. One could conjecture of orbits where the particles reach speed of light even before the collision. Such orbits, if they exist, are not studied here.

We start by some monotonicity properties. From Eq. (8) it follows that  $\frac{dv_1}{dt_1} < 0$  for all times, and by symmetry one also has  $\frac{dv_{2a}}{dt_{2a}} > 0$  and  $\frac{dv_{2b}}{dt_{2b}} > 0$ , such that we can establish that

$$|v_{2a}| < v_1 < |v_{2b}|; \quad (16)$$

for any time  $t_1$ : It is also easy to show that  $r_a(t_1)$  and  $r_b(t_1)$  are piecewise monotonic functions of  $t_1$ : From Eqs. (10), (12) and (13) it follows that

$$\frac{dr_a}{dt_1} = \frac{v_1 - v_{2a}}{1 + v_{2a}}; \quad (17)$$

and

$$\frac{dr_b}{dt_1} = \frac{v_1 - v_{2b}}{1 - v_{2b}}. \quad (18)$$

As the velocities are globally monotonic, there is a maximum radius  $r_0$  (see Figure 1) attained at  $t_1 = t_0 > t_c$ , when  $v_1(t_1 = t_0) = v_{2a}(t_{2a})$ , (and such that  $\frac{dr_a}{dt_1} \Big|_{t_1=t_0} = 0$ ). It must be that

$$\begin{aligned} \frac{dr_a}{dt_1} &> 0; \quad t_1 < t_0; \\ \frac{dr_a}{dt_1} &< 0; \quad t_1 > t_0; \end{aligned} \quad (19)$$

As the collision happens at  $t_1 = t_c < t_0$ , we can restrict to the increasing part of  $r_a$ ; ( $t_c < t < t_0$ ), an interval where Eq. (15) determines the bound

$$r_b(t) = r_a(t - t_c) < r_a(t); \quad (20)$$

For the complementary interval before the next collision ( $t_0 < t < t_c$ ), we have  $r_a < r_b$ . Because of inequality (20), when the largest radius  $r_a$  goes to zero,  $r_b$  must go to zero as well such that this largest radius becomes the natural control parameter for the dynamics in the neighborhood of the collision. In the following we show that velocities  $v_{2a}$ ;  $v_1$ ; and  $v_{2b}$  must all tend to the speed of light in modulus when this largest radius  $r_a$  goes to zero.

Lemma:

Assuming that a continuous solution  $(r(t); v(t))$  exists in an open neighborhood of the collision point  $r_a = 0$  and  $t = t_c$ , then we must have that both velocities go to the speed of light at  $t = t_c$

Proof by contradiction:

Dividing Eq. (8) by Eq. (18) we obtain an equation for the evolution of  $v_1$  with  $r_b$

$$\frac{dv_1}{dr_b} = \frac{(1 - v_b)}{2(v_1 - v_b)} \frac{(1 - v_a)}{r_a^2(1 + v_{2a})} + \frac{(1 + v_{2b})}{r_b^2(1 - v_b)} - 1 - v_1^2 \quad (21)$$

If neither of the velocities goes to the speed of light at the collision, then by Eq. (9) it must be that

$$v_1 = v^c < 1; \quad (22)$$

$$v_{2a} = v^c;$$

$$v_{2b} = v^c;$$

Given that the velocities are bounded according to Eq. (22) and because of Eq. (20), the second term on the right-hand side of Eq. (21) dominates and integration of this dominant term yields

$$v_1 = \frac{k}{r_b} + \dots \quad (23)$$

with  $k$  a nonzero constant. Equation (23) predicts that  $v_1$  becomes infinite as  $r_b$  goes to zero, an absurd, as we have assumed that  $v_1 = v_1^c < 1$ . We conclude that  $v_1(r_a = 0) = 1$  and  $v_{2b}(r_b = 0) = v_{2a}(r_a = 0) = 1$ .

### III. THE TIME TRANSFORMATION

To motivate our regularizing time-transformation, we assume that at least one regular orbit exists and construct its formal series expansion in the neighborhood of the collision. For this we develop the function  $1 + v_{2a}$  in a power series of  $r_a$  and the function  $1 + v_{2b}$  in a power series of  $r_b$

$$1 + v_{2a} = a_0 r_a^q + a_1 r_a^{q+1} + \dots \quad (24)$$

$$1 + v_{2b} = B_0 r_b^s + B_1 r_b^{s+1} + \dots \quad (25)$$

where  $s$  and  $q$  must be positive because the velocities have a bounded modulus ( $|v_j| < 1$ ) and  $a$  and  $B > 0$  are to be determined later. One can verify by simple substitution that the evolution parameter  $u$  defined as

$$dt_1 = du (1 + v_{2a})(1 - v_b); \quad (26)$$

regularizes Eqs. (10)–(14) and Eqs. (17)–(18) at the collision. The only problematic regularization left is the right-hand side of Eq. (8), which involves two indeterminate limits at the collision. In the following we show that the second term on the right-hand side of Eq. (8) vanishes at the collision. For this we divide Eqs. (8) and (18) by Eq. (17) and obtain differential equations for  $v_1$  and  $r_b$  in terms of the evolution parameter  $r_a$

$$\frac{dv_1}{dr_a} = \frac{(1 - v_1^2)^{3/2}}{2 r_a^2 (v_1 - v_a)} (1 - v_a) + \frac{(1 + v_{2b})(1 + v_{2a}) r_a^2}{r_b^2 (1 - v_b)} \quad (27)$$

$$\frac{dr_b}{dr_a} = \left( \frac{v_1 - v_b}{1 - v_b} \right) \left( \frac{1 + v_{2a}}{v_1 - v_a} \right) \frac{1 + v_{2a}}{2} + \frac{1 + v_{2a}}{2} \frac{a}{2} r_a^q + \dots \quad (28)$$

Eqs. (27) and (28) are converted into ordinary differential equations by use of the series of Eqs. (24) and (25). Integrating the leading term of Eq. (28) we find

$$r_b \sim \frac{a r_a^{q+1}}{2(q+1)} \quad (29)$$

To obtain a series for  $v_1$  from Eq. (27), we start by noticing that the first term on the right-hand side of Eq. (27) is approximately 2 in the neighborhood of  $r_a = 0$

$$(1 - v_a) \sim 2 \quad (30)$$

By use of Eqs. (24), (25) and (29) we can show that the second term of the right-hand side of Eq. (27) is proportional to  $r_a^{qs+s-q}$

$$\frac{(1 + v_{2b})(1 + v_{2a}) r_a^2}{r_b^2 (1 - v_b)} \sim r_a^{qs+s-q} \sim \frac{(1 + v_{2a})}{(1 + v_{2b})} \quad (31)$$

As the velocity is monotonic, the limit of the ratio  $\frac{(1 + v_{2a})}{(1 + v_{2b})}$  in Eq. (31) must either be zero or at the worst this limit can be a constant value, which implies that  $qs + s - q = 0$ . In the following we assume that Eq.(31) vanishes near the collision, and obtain a leading approximation to the equations of motion. This leading approximation in turn calculates  $qs + s - q = 3$ , showing that the assumption is consistent. The pathological option  $qs + s - q = 0$  must be analyzed separately, as then Eq. (31) has a finite limit. This analysis again determines that  $qs + s - q = 3$ , showing that a vanishing limit for Eq. (31) is the only consistent choice.

With the above in mind, the leading terms of Eqs. (8), (17) and (18) in the neighborhood

of  $u = 0$  are

$$\begin{aligned} \frac{dr_a}{du} &= 4; & (32) \\ \frac{dv_1}{du} &= \frac{4}{r_a^2} (1 - v_1)^{3-2}; \\ \frac{dr_b}{du} &= 2(1 + v_a): \end{aligned}$$

Choosing  $u = 0$  at  $t = t_0$  and using Eq. (24) to eliminate  $v_{2a}$ , Eqs.(32) can be integrated, yielding

$$r_a = 4u; \tag{33}$$

$$1 + v_{2a} = au^q \tag{34}$$

$$1 - v_1 = 32u^2; \tag{35}$$

$$r_b = \frac{2a}{(q+1)} u^{q+1}; \tag{36}$$

while Eq.(25) predicts the leading term

$$1 + v_{2b} = B \frac{2^s a^s B}{(q+1)^s} u^{s(q+1)}; \tag{37}$$

The last consistency condition on the solution is that  $x_{2a}(t)$  and  $x_{2b}(t)$  must describe the same orbit: This is accomplished if there exists a shift function  $u(u) > 0$ ; such that

$$t_1(u + u(u)) = t_{2a}(u); \tag{38}$$

and also

$$1 - v_1(u + u(u)) = 1 + v_{2a}(u); \tag{39}$$

$$1 + v_{2b}(u + u(u)) = 1 - v_1(u) \tag{40}$$

at  $u = 0$ : We can find from Eq. (33) that

$$u(u) = 2^{1-4} u^{\frac{1}{2}};$$

and also  $B = s = 2$ ;  $q = 1$  and  $a = 2^{\frac{p-2}{2}}$ : Finally we can express the velocities in terms of the radii using Eqs. (34) and (37)

$$1 + v_{2a} = \frac{p-2}{2} \frac{2}{r_a} + \dots; \tag{41}$$

$$1 - v_1 = 2 \frac{2}{r_a} + \dots; \tag{42}$$

$$1 - v_1 = \frac{p-2}{2} \frac{2}{r_b} + \dots; \tag{43}$$

$$1 + v_{2b} = 2 \frac{2}{r_b} + \dots; \tag{44}$$

and for later use the velocities  $v_{2a}$  and  $v_{2b}$  can be expressed as functions of  $v_1$

$$1 + v_{2a} = \frac{1}{2} \frac{v_1^2}{1 - v_1^2} + \dots \quad (45)$$

$$1 + v_{2b} = \frac{(1 - v_1^2)^2}{4} + \dots \quad (46)$$

For later use, it is interesting to obtain a further term of the series for  $v_1$ ; Eqs. (42) and (43) in the following way: By use of the leading terms of Eqs. (33)–(36) we can express Eq. (27) as

$$\frac{dv_1}{dr_a} = \frac{(1 - v_1^2)^{3/2}}{r_a^2 (1 + v_1)} + O(r_a^4) : \quad (47)$$

The solution of (47) with the condition that  $v_1 = 1$  at  $r_a = 0$  is

$$v_1(r_a) = \frac{(1 + C r_a)^2}{(1 + C r_a)^2 + r_a^2} + O(r_a^5) : \quad (48)$$

Expanding Eq. (48) in powers of  $r_a$  we obtain

$$1 - v_1 = 2r_a^2 + 4C r_a^3 + \dots \quad (49)$$

which exhibits the next term in the series of Eq. (42). An extra term in the series of Eq. (44) for  $v_{2b}$  can be obtained by replacing  $r_a$  by  $r_b$  and  $v_1$  by  $v_b$  in Eq. (49)

$$1 + v_{2b} = 2r_b^2 + 4C r_b^3 : \quad (50)$$

This symmetry along time-reversible orbits is illustrated in Figure 3 (i.e., that  $v_{2b}(r_b) = v_1(r_a = r_b)$ ). The constant  $C$  is related to the energy  $E$  of the orbit and is calculated in the next section. Last, it is of interest to notice that the term corresponding to the past in Eq. (27) contributes to the expansion of  $v_1$  only at 5th order in  $r_a$ :

#### IV. TWO FINITE VARIABLES DEFINED BY THE ENERGY

The conserved energy of the Kepler problem is simple and well known, while the corresponding energy for our relativistic problem is somewhat unfamiliar. The Poincare invariance of the Fokker Lagrangian determines a four-vector constant of motion, which involves an integral over a light-cone of the orbit [1,3]. For the one-dimensional symmetric motion

of equal masses, as explained in Ref. [3], the total energy  $E_T^{WF} = E_1 + E_2 = 2E$  can be simplified in two independent constants (a time-reversed pair,  $E_1 = E_2 = E$ )

$$E_1 = \frac{1}{1 - v_1^2} \frac{1}{2r_a} \frac{Y_a}{(1 + v_1)}; \quad (51)$$

$$E_2 = \frac{1}{1 - v_1^2} \frac{1}{2r_b} + \frac{Y_b}{(1 - v_1)}; \quad (52)$$

with  $Y_a$  and  $Y_b$  given by

$$Y_a = \frac{(1 + v_1)}{2} \int_{t_2a=t_1+r_a=c}^Z \frac{v_1}{r^2} \frac{1 + v_2}{1 - v_2}; \quad (53)$$

$$Y_b = \frac{(1 - v_1)}{2} \int_{t_2b=t_1-r_b=c}^{Z, t_1} \frac{v_1}{r_+^2} \frac{1 - v_2^+}{1 + v_2^+}; \quad (54)$$

where  $r_+; v_2^+$  and  $r_-; v_2^-$  stand for the radius and velocity at the advanced and retarded light-cones of particle 1 respectively, as illustrated in Figure 4. The total linear momentum of a symmetric orbit can be expressed as  $P_T^{WF} = P_1 + P_2 = 0$ ; with the time-reversed pair  $P_1$  and  $P_2$  given by

$$P_1 = \frac{v_1}{1 - v_1^2} \frac{1}{2r_b} \frac{1}{2} \int_0^{Z, t_2b} \frac{dt (1 - v_{2+})}{r_+^2 (1 + v_{2+})} - \frac{1}{2} \int_0^{Z, t_1} \frac{dt (1 - v_{2+})}{r_+^2 (1 + v_{2+})}; \quad (55)$$

$$P_2 = -P_1 = \frac{v_2}{1 - v_2^2} + \frac{1}{2r_a} \frac{1}{2} \int_0^{Z, t_1} \frac{dt (1 + v_1)}{r^2 (1 - v_1)} - \frac{1}{2} \int_0^{Z, t_2a} \frac{dt (1 + v_1)}{r^2 (1 - v_1)}; \quad (56)$$

where  $v_2(t_1) = v_1(t_1)$  and  $v_1$  and  $v_1^+$  stand for the velocity at the retarded and advanced light-cones respectively. Using the equation of motion (Eq. (8)) one can check that the time derivative of either Eq.(51) or (55) vanishes. This implies that  $\frac{dP_1}{dt_1} = \frac{dE_1}{dt_1} = 0$  along the motion. The same applies to Eq. (52), which is the time-reversed of Eq.(51), and also to Eq. (56), the time-reversed of Eq. (55). Notice that the energy Eqs.(51) and (52) have the correct Coulombian limit far away from the collision, as  $Y_a$  and  $Y_b$  vanish for large distances. Using the near-collision behavior of Sec. III one finds that  $Y_a$  and  $Y_b$  as defined by Eqs. (53) and (54) have finite limits at the collision. We already mentioned that Eqs. (8)–(14) are not regular at the collision, i.e. the right-hand sides involve subtractions of infinities, which are undefined operations. In the following we use the energy Eqs. (51) and (52) to obtain differential equations to replace Eqs. (8)–(14) and which are regular along the collision at  $t = t_c$  (and also along the symmetric collision at  $t = t_c$ ). The value of  $Y_b$  as defined by Eq. (54) can be approximated by elimination of  $dt$  using the dominant term of Eq. (8)

$$\frac{1}{2} \int_{t_2b}^{Z, t_1} \frac{v_1}{r_+^2} \frac{1 - v_2^+}{1 + v_2^+} dt_1^0 = \int_{v_{2b}}^{v_1} \frac{v_1}{(1 - v_1^2)^{3/2}} dv_1 + O(r_a^5); \quad (57)$$

Evaluating the integral on the right-hand side of Eq. (57) yields an approximation for  $Y_b$  near the collision

$$Y_b \approx \frac{p \sqrt{1 - v_1}}{1 + v_1} \approx \frac{(1 - v_1)}{1 - v_1^2} : \quad (58)$$

Substituting this expression into the energy Eq. (52) yields the approximation

$$E \approx \frac{1}{2r_b} + \frac{1}{1 - v_1^2} ; \quad (59)$$

which predicts the same behavior for  $v_{2b}(r_b)$  as Eq.(44): The near collision behavior of  $Y_a$  can be derived from Eq. (44)

$$Y_a \approx \frac{(1 + v_1)(r_a - r_b)}{2} \approx \frac{(1 + v_1) p \sqrt{1 - v_1}}{2 \sqrt{1 - v_1^2}} \quad (60)$$

Notice that we could have derived Eq.(44) from Eq. (58) with the assumption that  $Y_b$  is finite. In Sec. III we postulated that the advanced velocities had an ordered series to obtain Eq. (44). The fact that Eq. (44) can be obtained from the more elegant hypothesis that  $Y_b$  is finite all along the orbit suggests the natural mathematical space for a regular solution; the set of orbits with finite values for  $Y_a$  and  $Y_b$ . Using Eq. (52) and the approximations of Eqs. (48) and (43), the constant  $C$  can be calculated as

$$C = 2E : \quad (61)$$

The evolution of  $v_1$  respect to the parameter  $u$  can be calculated from Eq. (8)

$$\frac{dv_1}{du} = \frac{p \sqrt{1 - v_1^2}}{2} ; \quad (62)$$

where  $u$  is given by

$$1 - v_1^2 = \frac{(1 - v_{2a})(1 - v_{2b})}{r_a^2} + \frac{(1 + v_{2a})(1 + v_{2b})}{r_b^2} : \quad (63)$$

Notice the two numerically prohibitive features with Eqs. (62) and (63) : (i) Eq. (63) has indeterminacies of type  $\frac{0}{0}$ , and (ii) Eq. (62) does not evolve starting from the initial condition  $v_1 = 1$ . An alternative way to obtain  $v_1$  is to solve the energy Eqs. (51) and (52) for  $v_1$ . As the energy equations involve the variables  $Y_a$  and  $Y_b$ , it must be integrated along with equations for  $Y_a$  and  $Y_b$ : The needed equations of motion for  $Y_a$  and  $Y_b$  following from Eqs. (53) and (54) are

$$\frac{dY_a}{du} = \frac{(v_1 - v_{2a})(1 - v_{2b})(1 + v_1)}{2r_a^2} - \frac{v_1}{2(1 - v_1)} Y_a \frac{r \sqrt{1 - v_1}}{1 + v_1} ; \quad (64)$$

$$\frac{dY_b}{du} = \frac{(v_1 - v_{2b})(1 + v_{2a})(1 - v_1)}{2r_b^2} + \frac{v_1}{2(1 + v_1)} + Y_b \frac{r \sqrt{1 + v_1}}{1 - v_1} : \quad (65)$$

The system formed by Eqs. (64) and (65) still contains indeterminacies of type  $\frac{0}{0}$ , so we are not done yet.

In the following we show that the right-hand sides of Eqs. (64) and (65) both have a finite limit at the collision if: (i) the orbit has a finite energy and (ii) variables  $Y_a$  and  $Y_b$  as defined by Eqs. (53) and (54) are finite along the collision at  $t = t_c$ . It is convenient to define variables  $z = \frac{p}{1 - v_1}$  and  $w = \frac{p}{1 + v_1}$  plus two manifestly finite quantities and as

$$\begin{aligned} & \frac{1 + v_{2a}}{1 - v_1}; \\ & \frac{1 + v_{2b}}{(1 - v_1)^2}; \end{aligned} \quad (66)$$

Notice that  $z = 0$  and  $w = \frac{p}{2}$  at  $v_1 = 1$ , and the limit values of and at the collision as predicted by Eqs. (45) and (46) are:  $= 2$  and  $= 1=4$ . We can solve the energy Eq. (51) for  $r_a$  and the energy Eq. (52) for  $r_b$ , yielding

$$r_a = \frac{w^2 z}{2 (w^2 z E - z Y_a + w)} = \frac{w}{2} z; \quad (67)$$

$$r_b = \frac{z^2 w}{2 (z w E + w Y_b + z)} = \frac{z}{2} w; \quad (68)$$

The variables  $r_a$  and  $r_b$  as defined by Eqs. (67) and (68) have finite limit values at the collision,  $r_a^0 = 1$  and  $r_b^0 = 1$ . It is nice to observe that these finite limits are a consequence of  $E$ ,  $Y_a$  and  $Y_b$  being finite in (67) and (68). We arrive then at a concise definition of a regular orbit: one defined by finite values of  $E$ ,  $Y_a$  and  $Y_b$ . We can express Eq. (64) in terms of these finite quantities as

$$\begin{aligned} \frac{dY_a}{du} = & T_f^a + z \left[ 4 \frac{z}{a} + \frac{1}{2w} Y_a + 2w^2 \frac{Y_b}{b} - 4z^2 \frac{z}{a} + \right. \\ & \left. + z^3 \left[ 2 \frac{z}{a} - 2w^2 \frac{Y_b}{b} + 6z^4 \frac{z}{a} - 4z^5 \frac{z}{a} \right]; \right. \end{aligned} \quad (69)$$

where  $T_f^a$  is written finite explicitly by

$$T_f^a = \frac{16 (1 - z=2) (1 - \frac{z}{a})}{\frac{z}{a}} + \frac{4Y_b - z^3 w^2}{\frac{z}{b}};$$

At  $z = 0$  the only nonzero term on the right-hand side of Eq. (69) is

$$T_f^a = 4 (1 - z (w E - Y_a = w))^2;$$

which is finite at the collision ( $z = 0; w = 0$ ). Substitution of Eqs. (68) and (67) into Eq. (65) and some algebraic manipulations yield

$$\begin{aligned} \frac{dY_b}{du} = & T_b^f + \left[ 16 + \frac{1}{2w} + 8wE \frac{Y_b^2}{Y_b} - 4w \frac{Y_b}{\frac{2}{a}} + \frac{8}{w} Y_a Y_b^2 + \right. \\ & + z \frac{8}{w Y_b} \left[ 8E Y_a Y_b^2 - 16wE + 2 \frac{Y_b^2}{\frac{2}{b}} - 4w^2 E^2 Y_b^2 - \frac{4}{w^2} Y_a^2 Y_b^2 \right] \\ & + z^2 \left[ 2w^3 \frac{Y_b^2}{\frac{2}{b}} - \frac{16E}{Y_b} - \frac{1}{2w} \right] \\ & \left. + z^3 \left[ 8w \frac{E^2}{Y_b} - 8w \frac{Y_b}{\frac{2}{a}} + 2 \frac{Y_b^2}{\frac{2}{b}} + 4w z^4 \frac{Y_b}{\frac{2}{a}} \right]; \right. \end{aligned} \quad (70)$$

where

$$T_b^f = \frac{4Y_b}{z} (2w - Y_b); \quad (71)$$

The term  $T_b^f$  defined by Eq. (71) was singled out in Eq. (70) because it contains a division by zero, and is the only part of Eq. (70) that could in principle be singular. To show that  $T_b^f$  has a finite limit along an orbit of finite energy, we first use the energy Eq. (52) to express  $z$  as

$$z = \frac{r_b + \frac{p}{r_b} \sqrt{2w^2 Y_b + r_b + 4w^2 E Y_b r_b}}{w (1 + 2E r_b)}; \quad (72)$$

Substituting the approximation of Eq. (58) for  $Y_b$

$$Y_b \approx \frac{p}{2} \left( \frac{z}{w} + O(z^4) \right);$$

into Eq. (72), we find the expansion for  $z^2$  ( $r_b \ll 1$ ) to be

$$z^2 = 2r_b \frac{p}{2} - \frac{p}{4} \frac{p}{2E r_b^2} + O(r_b^3) \quad (73)$$

Last, as discussed above Eq. (50) and illustrated in Figure 3, the particle exchange symmetry along symmetric orbits implies that the function  $v_1(r_b)$  is equal to the function  $v_b(r_a)$ . Changing the argument of Eq. (73) from  $r_b$  to  $r_a$  and eliminating this  $r_a$  in favor of  $v_1$  with Eq. (42) we obtain

$$\frac{1 + v_{2a}}{z} = 2 \frac{p}{2} \frac{p}{2E} z + O(z^2) \quad (74)$$

Substituting Eq. (74) for  $z$  into the formula for  $T_b^f$ , Eq. (71), and expanding we can determine that  $T_b^f$  is finite and nonzero at the collision.

V . NUMERICAL CALCULATIONS WITH THE REGULARIZED EQUATIONS

We shall use here a numerical method previously developed by us in Ref.[7] for the repulsive case. We start by postulating  $v_{2a}$  and  $v_{2b}$  as two arbitrary power series like Eqs. (24) and (25). Next we integrate the regular equations (69) and (70) together with Eqs. (10)–(14) written in terms of the variable  $u$  of Eq. (26), which predicts future and past trajectories for particle 2,  $x_{2a}(t_2)$  and  $x_{2b}(t_2)$ . Next we use a minimization scheme to modify the coefficients of Eqs. (24) and (25) to improve the consistency of the two histories, until the eventual convergence to a consistent history for particle 2 is reached. Some observations are in order: (i) The behavior of  $v_{2a}$  near the collision must be that of Eq. (74). (ii) To describe a symmetric orbit in the most economical way, the global time-reversal symmetry can be embedded in the ansatz for the velocities (ansatz is defined here by a postulate like Eqs. (24) and (25)). According to this time-reversal symmetry, the advanced and retarded velocities must satisfy

$$v_{2a}(t) = v_{2b}(t);$$

$$r_a(t) = r_b(t);$$

To satisfy (i) and (ii) and the near-collision behavior of Eqs. (41)–(46) we use a variant of Eqs. (24) and (25) that postulates  $v_{2b}$  and  $v_{2a}$  defined by an arbitrary function  $(r_a; r_b)$  such that

$$\frac{1 - v_{2a}}{1 + v_{2a}} = \frac{2}{(3 + v_1)} \frac{r}{1 + v_1} \frac{r_a^2}{r_b} (r_a; r_b); \quad (75)$$

$$\frac{1 + v_{2b}}{1 - v_{2b}} = \frac{2}{(3 - v_1)} \frac{r}{1 - v_1} \frac{r_b^2}{r_a} (r_b; r_a); \quad (76)$$

If  $(r_a; r_b)$  is regular and evaluates to one at the collision, the above ansatz of Eqs. (75) and (76) guarantees that  $T_b^f$  defined by Eq.(71) is explicitly finite (i.e. there is no division of zero by zero to spoil the numerical calculations). Notice that under time reversal  $r_a$  and  $r_b$  are interchanged ( $r_a \leftrightarrow r_b$ ) and  $v_1$  is exchanged by  $-v_1$  ( $v_1 \leftrightarrow -v_1$ ), such that the right-hand sides of Eqs. (75) and (76) are exchanged. This is the embedding of the time-reversal symmetry  $v_{2a} \leftrightarrow -v_{2b}$ . Last, the near-collision behavior of Eqs. (45) and (46) is also built into formulas (75) and (76). For numerical convenience, the function  $(r_a; r_b)$  must be postulated in two different ways depending on the energy of the orbit:

(I) A rational Pade approximation defined as

$$(r_a; r_b) = \frac{1 + K_1 r_b + K_2 r_b^2 + \dots + K_N r_b^N}{1 + k_1 r_a + k_2 r_a^2 + \dots + k_N r_a^N} : \quad (77)$$

Notice that Eq.(77) is a quotient of a polynomial on  $r_b$  over a polynomial on  $r_a$ , which again is need to make  $T_b^f$  of Eq.(71) explicitly finite one the first collision and  $T_a^f$  finite at the next collision (which exchanges  $r_a$  and  $r_b$ )

(II) A difficult limit for the above approximation are the orbits with an energy very close to one ( $E \approx 1$ ), which is the atomic energy range. because the function jumps abruptly from the value of one to the constant value at the Coulombian limit ( $r_a \approx r_b \approx 1$ ): The numerically correct procedure for shallow energies is to postulate  $v$  with Spline interpolation [23] on the interval  $1 < v < 1$ , defined such that  $v = 1$  at the collision ( $v = 1$ ) and such that  $T_a^f$  and  $T_b^f$  are finite at both collisions. This is accomplished with the definition

$$1 + \frac{P}{1 - v^2} P(v) : \quad (78)$$

We use up to 22 intervals to approximate the function  $P(v)$  with Splines[23]. Either the coefficients  $k_1 \dots k_N; K_1; \dots K_N$  of the Pade approximation or the polynomial coefficients  $c_i$  of the cubic Splines are to be determined by the self-consistent minimization in each case. After these are substituted into Eqs. (75) and (76), and these into Eqs. (69) and (70), our regular equations of motion become ordinary differential equations that are integrated with a standard 9/8 explicit Runge-Kutta pair, generating the future and past of particle 2. Our self-consistent method calculates two functions that should vanish along a symmetric orbit

$$S_1(k;t) = x_1(t) + x_{2a}(t) ; \quad (79)$$

$$S_2(k;t) = x_1(t) + x_{2b}(t) ;$$

at about  $m$  points along the orbit ( $m \approx 400$ ): The interpolation coefficients (either  $k_i; K_i$  or  $c_i$ ) are changed by a least-square minimization algorithm (Levenberg-Marquardt algorithm) [24]. Notice that if we could find an analytical solution for the orbit, these coefficients could be calculated by setting  $S_{1,2}$  to zero. In practice we determine a numerical zero for  $S_{1,2}$  of size  $1 \times 10^{-5}$  (see Table 1). As discussed below Eq. (46), only at  $O(r_a^5)$  the information of the past becomes important near the collision, such that we should use  $N \approx 5$ ; to include past information into Eq. (27).

We are now ready to start the integrations from  $r_a = r_b = 0$ ; using the approximate coefficients and  $E$  already calculated. The complete set of equations includes Eqs. (65) and (64) together with Eqs. (10)–(14) in terms of  $r_a; r_b; Y_a$  and  $Y_b$ : The initial condition  $r_a = 0; r_b = 0; v = 1$ ; expressed in terms of the regular variables reads

$$\begin{aligned} Y_a(u=0) &= 0; \\ Y_b(u=0) &= \frac{p}{2}; \end{aligned} \tag{80}$$

The energy  $E$  is a parameter that appears explicitly in the regular equation of motion, and the numerical procedure fixes  $E$  while the interpolation coefficients are adjusted by the minimization scheme. The velocity  $v_1$  is calculated numerically by solving Eqs. (51) and (52) for  $v_1$ : The numerically calculated orbits using the Pade approximation of Eq. (77) are shown in Figure 5 for four different energies ( $E = 1.0; E = 0.1; E = 0.5$  and  $E = 0.8$ ). In Table 1 we list the quantities related to these numerically calculated orbits. Notice in Table 1 that the energy becomes negative when the maximum light-cone radius is lesser than the classical electronic radius. The orbits at atomic energies ( $E \leq 1$ ) have two clearly separated regions: (i) a near-collision region where the velocity is very close to one and (ii) the turning region, where  $r_a \approx r_b \approx 1$  and  $v \approx \frac{3}{2}$ . This last segment of such orbits approximates the turning region of Coulombian orbits. Of course in the collision region these can never be equal, as  $v_1 \neq 1$  for Coulombian orbits. The transition between these two regions is abrupt, as illustrated in Figure 6. In Figure 7 we magnify the region of discontinuity for various energies, illustrating that the discontinuity in  $v$  changes shape with increasing  $E$ : In Figure 8 we show the numerically calculated orbits using the Spline interpolation for  $v$  (Eq. (78)). The energy  $E$  and the relative error of these atomic orbits are shown in Table 2. Notice in Table 2 that the value of  $r$  is converging to  $3=2$  as it should for Coulombian orbits.

## V I. C O N C L U S I O N S A N D D I S C U S S I O N

We derived a differential equation that is regular along the collision of two equal masses with attractive interaction of the action-at-a-distance electrodynamics, allowing the numerical study of these orbits for the first time. Our regular numerical method starts the

integration exactly from the collision. Our procedure is not covariant because we restricted the work to symmetric orbits, having the energy as the only free parameter (the other parameter should be the Lorentz boost parameter). A covariant treatment shall be left for future work, along the lines of Appendix B of Ref. [7]. In this Appendix we discuss that, for the equal-mass only, a symmetric orbit is defined in any Lorentz frame by the covariant condition that the future of one particle is the past of the other. The numerical results of Ref. [7] suggest that at least for the repulsive equal-mass case a boosted symmetric orbit is already the general nonrunaway solution. The generalization of this numerical study to the attractive case awaits a covariant regularization.

Some failed attempts taught us that the different-mass attractive case is far more complex, and possibly not even regularizable. At present we do not even know how to coin a formal series solution near the collision for this case. One of the reasons for that is that the energy expressions analogous to Eqs.(51) and (52) are far more complex. This fact confuses the definition of the finite variables analogous the definitions of Eqs. (53) and (54) for this case. This curious non-regularizability deserves further study.

The two-body problem with repulsive interaction also displays a singularity at high energies, but surprisingly enough this is not because the particles collide (they never do). The singularity appears in the right-hand side of Eq. (2) when the particles come to the speed of light (the denominator containing  $(1 - v)$  vanishes). It was found by several authors, first in Ref. [25] and later in Ref. [21], that particles reach the speed of light and turn back keeping a minimum distance of approximation of about one classical electronic radius. The regularization of this problem shall be published elsewhere [26]. This minimum distance of closest approach of about one classical electronic radius is a kind of exclusion principle of the action-at-a-distance theory. It is of interest to notice that this exclusion behavior is already found with the post-Galilean low-velocity approximation to the Fokker Lagrangian, the Darwin Lagrangian [2]; The algebraic-differential equations of motion of the Darwin Lagrangian were studied analytically in [27] and the phenomenon of closest approximation was discovered. The distance of closest approximation is found to be exactly the classical electronic radius.

V II. A P P E N D I X A : T H E L E V I - C I V I T A R E G U L A R I Z A T I O N

We shall briefly review the Levi-Civita regularization of the Galilei-invariant Kepler problem in the plane [46] and compare it to the regularization of our Poincaré-invariant Kepler problem. A consequence of the Galilei invariance of the Kepler problem is that the Equations of motion separate in two independent blocks: one Equation for the motion of the center-of-mass vector  $X = (m_1 x_1 + m_2 x_2)/M$  and another for the motion of the relative vector  $x = x_1 - x_2$

$$M \ddot{X} = 0; \tag{81}$$

$$\ddot{x} = -\frac{e^2 x}{r^3}; \tag{82}$$

where  $r = |x|$  stands for the Euclidean modulus of the relative vector  $x$  and  $\mu$  and  $M$  are the reduced mass and the total mass respectively. We notice that Eq. (82) is singular at  $r = |x| = 0$  and a numerical method based on it is bound to fail. The first step of the Levi-Civita regularization for collision orbits was pointed by Euler [28] and consists of a change of the evolution parameter from time to a parameter  $s$  defined by

$$dt = r ds; \tag{83}$$

whereby each time-derivative in Eq. (82) is replaced by

$$\frac{d}{dt} = \frac{d}{r ds}; \tag{84}$$

It is also convenient to describe the relative vector by a complex number  $z$  defined such that

$$z^2 = x + iy; \tag{85}$$

where  $x$  and  $y$  are the Cartesian components of the vector  $x$ . Eq. (82) defines the evolution of  $z$  in terms of  $s$  as

$$\left(\frac{2z}{r^2}\right) \left(\frac{d^2 z}{ds^2} - \frac{E}{2} z\right) = 0; \tag{86}$$

where  $E$  stands for

$$E = -\frac{1}{2} \left( \dot{x}^2 + \dot{y}^2 \right) - \frac{e^2}{r}; \tag{87}$$

Without further information, formula (87) in Eq. (86) stands for a difference of two infinities at  $r = 0$ , a numerically prohibitive feature. With the recognition that  $E$  is a constant of

motion, it can be replaced by a constant real number in the numerical procedure, and Eq. (86) becomes the regular Equation of a harmonic oscillator. This second and crucial step completes the Levi-Civita regularization of the Kepler problem.

As the collision orbit of the Kepler problem is not so familiar, let us solve for it explicitly. In general Eq.(86) is an equation for a complex number, but as we want  $y = 0$ , because of (85) we only need a real solution. Eq.(86) requires that

$$\frac{d^2 z}{ds^2} - \left(\frac{E}{2}\right)z = 0; \quad (88)$$

for all points but the origin. The periodic real solution that passes by  $r = 0$  at  $s = 0$  is

$$z_r = A \sin(ks); \quad (89)$$

where  $k = \sqrt{E/2}$ ; The dependence of  $A$  on the energy can be found by substitution of Eq. (84) into Eq. (87), yielding

$$E = \frac{2k^2 A^2 \cos^2(ks) - e^2}{A^2 \sin^2(ks)};$$

which determines  $A = \sqrt{\frac{e^2}{E - k^2}}$ . Some observations are in order: (i) Once Eq. (86) holds for any planar orbit, all  $l \neq 0$  angular momentum orbits are ellipses with the motion along the  $x$  axis approximated by (89) and with the motion along the  $y$  axis described by another harmonic function of size  $l$ : This  $y$  coordinate is controlled by the  $l$  imaginary part of  $z$  via (85) (notice that for physical orbits  $E$  is real, such that  $z_r$  satisfies an uncoupled harmonic equation like (88)). (ii) The collision orbit is the "limit" of a zero angular momentum ellipse. In this limit the focus of the ellipse tends to the center of force, and the velocity turns around it almost discontinuously from minus to plus infinite along the  $x$  direction. This is the "collision" with the singularity. At variance, in the present relativistic case the derivative of the velocity vanishes at the collision, and therefore the next segment of the orbit "passes through" the center of force and continues with the speed of light to the other side. This topological difference between the Galilei and Poincare invariant cases is unimportant to construct one-dimensional orbits, as we can concentrate in the unit cell of the orbit between two consecutive collisions, but it might prove important for planar orbits.

Acknowledgments: E. B. Hollander acknowledges a Fapesp PhD scholarship, proc. 99/08316-8 and J. De Luca acknowledges CNPQ, Brazil.

## IX . FIGURE CAPTIONS

Fig. 1 A symmetric trajectory, arbitrary units. Indicated are the maximum light-cone distance  $r_0$ , the velocity  $v_1$  of particle 1 at time  $t_1$  and the corresponding retarded and advanced velocities of particle 2,  $v_{2b}$  and  $v_{2a}$ . The trajectories of particle 1 (solid line on the right-hand side) and particle 2 (solid line on the left-hand side) are illustrated from the outgoing collision at  $t = t_e$  until the ingoing collision at  $t = t_c$ :

Fig. 2 The orbits of particle 1 (solid line on the right-hand side) and particle 2 (solid line on the left-hand side) in arbitrary units. Indicated is the symmetric point  $v_1 = 0$  at  $t = 0$ . Also shown are the velocity  $v_1$  of particle 1 at time  $t_1$  and the corresponding retarded and advanced velocities  $v_{2b}$  and  $v_{2a}$  of particle 2:

Fig. 3 A symmetric orbit in arbitrary units. The symmetric orbit is completely defined by only two functions  $r(t)$  and  $v(t)$ , from which the quantities  $r_a$ ;  $r_b$ ;  $v_1$ ,  $v_{2b}$  and  $v_{2a}$  are determined. Notice that  $v_a$  when  $r_b = r$  is the same as  $v_1$  when  $r_a = r$ .

Fig. 4 A symmetric orbit in arbitrary units. Illustrated are the segments of trajectory relevant to the evaluation of  $Y_a$  and  $Y_b$  and the quantities  $r^+$ ;  $r^-$ ;  $v_2^+$  and  $v_2^-$ .

Fig. 5 Numerically calculated trajectories using the Pade approximation, in units where  $c = e = m = 1$ . For each value of the energy  $E$ , the regularized integrator starts from the initial condition  $r_a = r_b = 0, v_1 = 1, Y_a = 0$  and  $Y_b = \frac{P}{2}$ : The four different orbits shown have energies  $E = 1.0, 0.1, 0.5$  and  $0.8$  as indicated.

Fig. 6. Numerically calculated  $\langle v_1 \rangle$  (as defined by Eq. (77)) plotted versus the velocity  $v_1$ , in units where  $c = e = m = 1$ . This figure illustrates the jump in  $\langle v_1 \rangle$  near  $v = 1$  at  $E = 0.8$  (Dash Dot),  $E = 0.9$  (Dot),  $E = 0.95$  (Dash) and  $E = 0.99$  (solid line).

Fig. 7. Numerically calculated  $\langle v_1 \rangle$  (as defined by Eq. (77)) plotted versus the velocity  $v_1$ , in units where  $c = e = m = 1$ . In this figure the discontinuity region near  $v = 1$  is

blown-up. Energies are  $E = 0.8$  (Dash Dot),  $E = 0.9$  (Dot),  $E = 0.95$  (Dash) and  $E = 0.99$  (solid line). Notice that the jump in  $\langle v \rangle$  at  $E = 0.99$  is quite differently from the jump at the other energies.

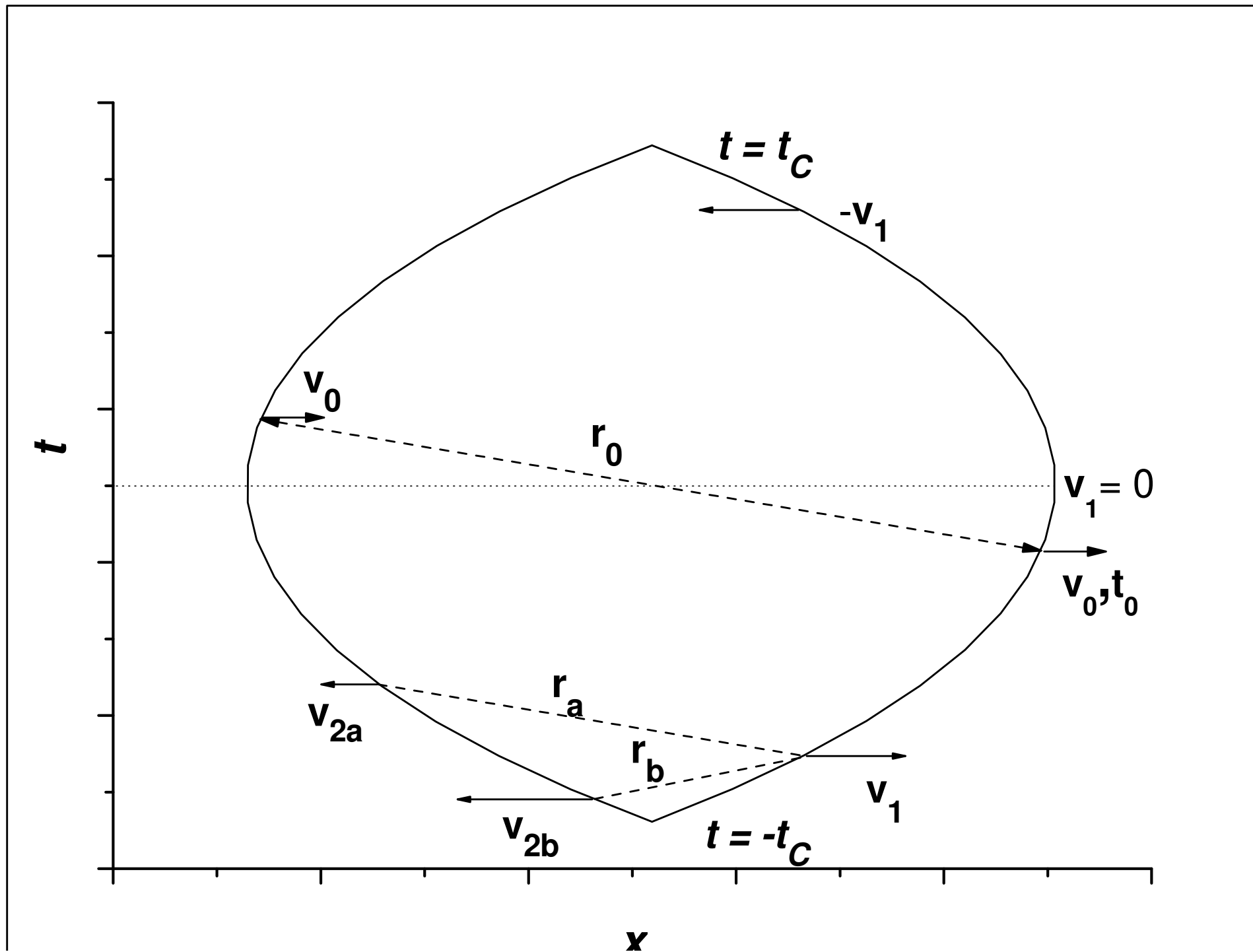
Fig. 8 Numerically calculated trajectories using the Spline interpolation, in units where  $c = e = m = 1$ . For each value of the energy  $E$ , the regularized integrator starts from the initial condition  $r_a = r_b = 0, v_1 = 1, Y_a = 0$  and  $Y_b = \frac{P}{2}$ : The four different orbits have energies  $E = 0.8, 0.9, 0.95$  and  $0.99$  as indicated.

Table 1: Numerically calculated orbits using the Pade approximation. Indicated are the energy  $E$ , the maximum light-cone distance  $r_0$  and the relative size of the first and last Pade coefficients, as well as the relative error of the minimization scheme,  $\epsilon = r_0$ . Notice that at the negative energy  $E = -1.0$  the maximum radius  $r_0$  is less than the classical electronic radius  $r = \frac{e^2}{m c^2} = 1$ .

Table 2: Numerically calculated orbits using the Spline interpolation. Indicated are the energy  $E$ , the maximum light-cone distance  $r_0$ , the saturation value  $r_0(v = 0)$  and the relative error of the minimization scheme,  $\epsilon = r_0$ . Notice again that at  $E = -1.0$  the maximum radius  $r_0$  is less than the classical electronic radius  $r = \frac{e^2}{m c^2} = 1$  and that  $r_0(v = 0)$  approximates the Coulombian limiting value of  $3/2$  as  $E$  tends to  $1$ :

- 
- [1] J.A. Wheeler and R.P. Feynman, Rev. Mod. Phys. 17, 157 (1945) ; 21,425 (1949).
  - [2] J.L. Anderson, Principles of Relativity Physics, Academic press, New York 1967, page 225.
  - [3] S. Klimenko and I. Nikitin, Il Nuovo Cimento 116 1029 (2001).
  - [4] T. Levi-Civita, Ann. Math. 9 1 (1903).
  - [5] E.L. Stiefel and G. Scheifele, Linear and Regular Celestial Mechanics Springer (1971) Berlin.
  - [6] S.J. Arseth and K. Zare, Celestial mechanics 10, 185 (1974).
  - [7] E.B. Hollander and J. De Luca, Phys. Rev. E 67, 026219 (2003).
  - [8] K. Schwarzschild, Göttinger Nachrichten, 128,132 (1903).
  - [9] H. Tetrode, Zeits. f. Physik 10, 137 (1922), A.D. Fokker, Zeits. f. Physik 58, 386 (1929).
  - [10] D. Leiter, Am. J. Phys. 38, 207 (1970).

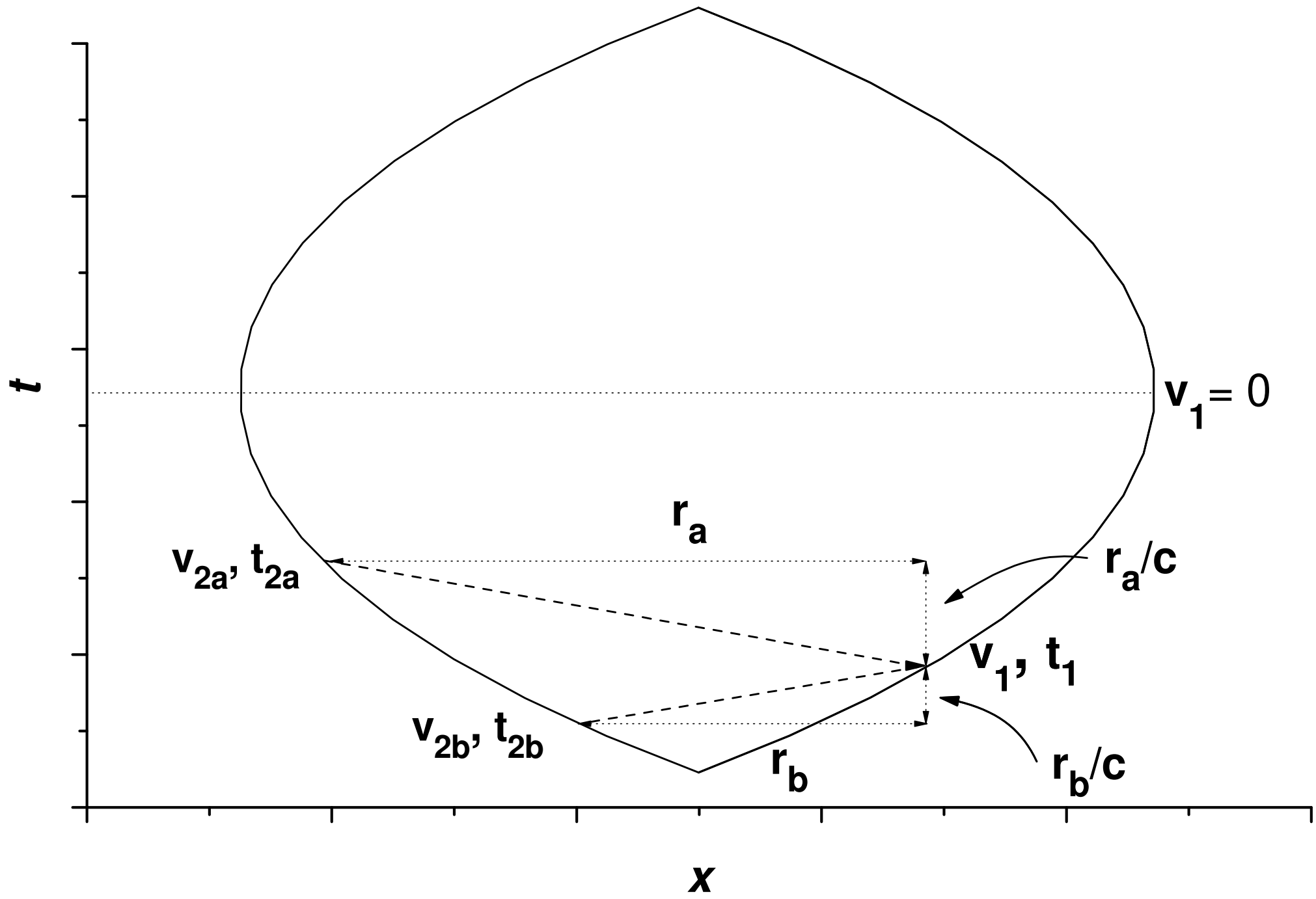
- [1] P A M Dirac, *Proceedings of the Royal Society of London, ser. A* 167, 148 (1938).
- [2] F Hoyle and J.N arlikar, *Cosmology and Action at a Distance Electrodynamics*, World Scientific Publishing, Singapore (1996).
- [3] J. Mehra *The Beat of a Different Drum : Life and science of Richard Feynman*, Oxford University Press, Oxford (1994), (chapter 5).
- [4] A .Staruskiwicz, *Annalen der Physik* 25, 362 (1970).
- [5] J A M urdock, *Annals of Physics* 84, 432 (1974).
- [6] R .D .D river, *Phys. Rev. D* 19, 1098 (1979). J. Hoag and R .D .D river, *Nonlinear Analysis, Theory, Methods & Applications* 15, 165 (1990).
- [7] M .Schonberg, *Phys. Rev.* 69, 211 (1946).
- [8] A .Schild, *Phys. Rev.* 131, 2762 (1963), A .Schild, *Science* 138, 994 (1962).
- [9] C .M .A ndersen and H .C .V on Baeyer, *Phys. Rev. D* 5, 802 (1972).
- [20] C .M .A ndersen and H .C .V on Baeyer, *Phys. Rev. D* 5, 2470 (1972).
- [21] S.V .K lin enko, I N N ikitin and W .F .U razm etov, *International Journal of Modern Physics C* 10, 1 (1999).
- [22] I. N .N ikitin and J .D e Luca, *International Journal of Modern Physics C* 12, 739 (2001).
- [23] H .A kim a, *Journal of the Association for Computing Machinery* 17, 589 (1970), G isela Engel-  
M ullges and Frank U hlig, *Numerical Algorithms with Fortran*, Springer, Berlin (1996).
- [24] J.C N ash, *Compact Numerical methods for Computers*, IOP publishing Ltd and Adam Hilger, Bristol and New York (1990).
- [25] R .N .H ill and E .kerner, *Relativistic Action-at-a-D istance: Classical and Quantum Aspects*, Lecture Notes in Physics, Edited by J.L lsa, pag. 129, Springer, Berlin (1982).
- [26] E .B uksm an and J .D e Luca, to be published
- [27] E .L aserra, I.P .P avlotsky and M .S trianese, *Physica A* 219, 141 (1995).
- [28] L .E uler, *Nov.Com m .Petrop.* 11, 144 (1765).





$E$	$r_0$	$k_1 r_0$	$K_1 r_0$	$k_5 r_0^5$	$K_5 r_0^5$	relative error
-1.0	0.2331	$-2.872 \times 10^{-2}$	$-1.714 \times 10^{-2}$	0.2625	$-6.8096 \times 10^{-2}$	$5 \times 10^{-5}$
0.1	0.5218	$-1.937 \times 10^{-2}$	$-4.7234 \times 10^{-2}$	-0.1646	0.3780	$1 \times 10^{-4}$
0.5	0.9275	$1.8971 \times 10^{-2}$	3.1345	-2.085	-1.782	$2 \times 10^{-4}$
0.8	1.821	$9.1806 \times 10^{-2}$	9.1063	-1.3304	0.3522	$6 \times 10^{-4}$







$E$	$r_0$	$r_0\theta(v_1 \approx 0)$	relative error
0.8	1.810	0.75	$2 \times 10^{-4}$
0.9	4.003	1.02	$3 \times 10^{-4}$
0.95	8.125	1.25	$5 \times 10^{-4}$
0.99	13.35	1.34	$3 \times 10^{-3}$



